Microporous and Mesoporous Materials 196 (2014) 1–7

Contents lists available at ScienceDirect

Microporous and Mesoporous Materials

journal homepage: www.elsevier.com/locate/micromeso

A new hierarchical porous zirconium phosphate membrane and its adsorption properties

Abubaker Abutartour, Yunjie Jia, Lotfia El Majdoub, Qinghong Xu *

State Key Laboratory of Chemical Resource Engineering, Beijing University of Chemical Technology, 15 Beisanhuan Donglu, Beijing 100029, PR China

A R T I C L E I N F O

Article history:
Received 19 January 2014
Received in revised form 24 April 2014
Accepted 28 April 2014
Available online 9 May 2014

Keywords:
Porous membrane
Organic zirconium phosphate
Si–O bridged
Adsorption

A B S T R A C T

A hierarchical porous zirconium phosphate membrane was prepared from bis(hexamethylenetriamine-penta(methylenephosphonic acid)), $ZrOCl_2{\cdot}8H_2O$, SiF_4 and hexadecyl trimethyl ammonium bromide. The membrane contains macropores of 200 nm in diameter, and mesopores of 19.2 nm in diameter. The membranes pores were bridged and limited by $(\text{–Si–O–})_n$ edges. The porous membrane exhibited high efficiency in removing Pb^{2+} and Cu^{2+} from wastewater.

1. Introduction

An important application of hybrid porous materials is adsorption and separation [1–4]. Numerous porous organic–inorganic hybrids have recently been developed for removing heavy metal ions, particularly Cd^{2+}, Cu^{2+}, and Pb^{2+}, from wastewater [5,6]. Organic functionality in porous materials can play an important role in their coordination with metal ions [7]. Thiols, thiourea and amines have been used as metal ion-binding motifs in mesoporous silica, and titanium phosphonate, for the efficient removal of Hg^{2+}, Cu^{2+}, and Cd^{2+} [8–11].

Phosphinic acid has been widely used in many fields since Horiguchi and Kandatsu first obtained C–P compounds from biological samples more than 50 years ago [12]. The hydroxyl functionality of phosphoric acid is easily substituted, and phosphinic acids with a wide variety of functionality have been prepared [13,14]. A large structural distortion occurs when the P–OH bond of metal phosphates is substituted by organic functional groups. This can significantly affect the electron cloud density P atoms in the framework.

Phosphinic acid is more suitable for preparing compounds with open frameworks than phosphoric acid, owing to its simultaneous collection of inorganic oxide and organic functional groups. The ability to introduce varying organic groups can yield materials with tunable structures. Open metal phosphate structures can be considered as materials between zeolites and organic metals. Metal phosphates are inorganic–organic hybrids, with applications in insertion chemistry, proton conductors, catalysis, and ion exchange [15,16].

Bis(hexamethylenetriaminepenta(methylenephosphonic acid)) (BMTPA) is a water treatment reagent with the molecular structure shown in Scheme 1. BMTPA can act as an organic phosphate source in the synthesis of organic zirconium phosphates, to give open porous structures. In the current study, the porous hexagonal organic zirconium phosphate membrane (BHAZP) is synthesized by autoclaving in the presence of BMTPA, $ZrOCl_2{\cdot}8H_2O$ and SiF_4. It is interesting that SiF_4 plays an important role in the synthesis, and the porous hexagonal membrane could not be formed without participation of SiF_4. Structure of $(\text{–Si–O–})_n$ is found at the edges and knots between the hexagonal plates, suggesting that the porous membrane is possibly formed based on the silicon atoms and limited in the area of $(\text{–Si–O–})_n$ hexagon framework (formation of $(\text{–Si–O–})_n$ hexagon framework is earlier than the structure of zirconium phosphate). Such a stepwise assembly to form porous membranes has not been previously reported. BHAZP contains macropores and mesopores, with diameters of approximately 200 and 19.2 nm, respectively, and the mesopores exist in the walls of the macropores. BHAZP has a surface area of $\sim$128.6 m^2/g, and exhibits good performance in the removal of Pb^{2+} and Cu^{2+} from wastewater. Its maximum Pb^{2+} adsorption capacity is 469.39 mg/g, higher than that of common inorganic adsorbents such as zirconium phosphate (α-ZrP, 400.01 mg/g) [17] and activated carbon (17.51 mg/g) [18] under similar conditions. The Cu^{2+} adsorption capacity of BHAZP is 310 mg/g, which is greater

---

* Corresponding author. Tel.: +86 10 64425037; fax: +86 10 64425385.
E-mail address: xuqh@mail.buct.edu.cn (Q. Xu).

http://dx.doi.org/10.1016/j.micromeso.2014.04.054
1387-1811/

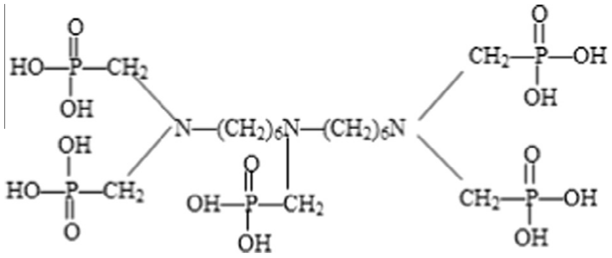

Scheme 1. Molecular structure of BMTPA.

than that of polycarboxylated starch (128.3 mg/g) [19], which is the largest previously reported Cu^{2+} adsorption capacity.

2. Experimental

All chemicals were of analytical grade and obtained from commercial suppliers, and were used without further purification. Zirconium dichloride oxide octahydrate ($ZrOCl_2{\cdot}8H_2O$) and BMTPA were obtained from Sinopharm Chemical Reagent Co. (PR China). Silicon tetrafluoride (SiF_4) and hexadecyl trimethyl ammonium bromide (CTAB) were purchased from Beijing Chemical Regent Co. (PR China).

2.1. Synthesis of BHAZP

Solutions of 0.30 M $ZrOCl_2$, 0.60 M BMTPA, and 0.60 M CTAB were prepared by dissolving the corresponding reagents in deionized water. A given amount of SiF_4 was added to the $ZrOCl_2$ solution. This solution was slowly added to the BMTPA solution under vigorous stirring and a slow N_2 flow, leading to a white suspension. The mixture was refluxed at 80 °C for 2 h, and then sealed in a polytetrafluoroethylene-lined autoclave and heated at 80 °C for 24 h. The product was obtained by centrifuging, thoroughly washing with deionized water and drying at 70 °C. The porous structure was produced after CTAB was extracted by refluxing in ethanol for 24 h.

2.2. Metal ion adsorption

Metal ion adsorption by BHAZP was characterized by testing in batch mode in 250-mL glass bottles. 0.10 g of BHAZP was added to 100-mL solutions containing varying concentrations of $Pb(NO_3)_2$ and $Cu(NO_3)_2$ (50–900 ppm). The mixtures were stirred at room temperature (25 ± 2 °C) for 24 h to ensure sorption equilibrium. The adsorbed metal ion contents were determined by atomic absorption spectroscopy on an Agilent 4510 spectrometer. Adsorption capacities were calculated from the concentration before and after adsorption of different concentrations of solutes [20]:

$$q_e = (c_0 - c_e)V/W \quad (1)$$

where q_e is the concentration of adsorbed solute (mg/g), c_0 and c_e are the initial and final concentrations of metal ions in solution (ppm), respectively, V is the solution volume (mL) and W is the mass of the adsorbent (g).

2.3. Characterization

Crystal structures were determined by powder X-ray diffraction (PXRD), using a Rigaku D/MAX diffractometer (made in Japan) with Cu K_α radiation (λ = 0.15406 nm, scanning speed = 10°/min). Fourier transform-infrared (FT-IR) spectra was recorded from KBr pellets (1 mg of sample to 100 mg of KBr) over the range of 400–4000 cm^{-1}, at 2 cm^{-1} resolution using a Bruker Vector-22 spectrometer (made in Germany). Zr and P contents were determined by inductively coupled plasma (ICP) spectroscopy, using a Perkin–Elmer plasma 40 emission spectrometer (made in Japan). C, H, O, and N contents were determined using a Vario-EL elemental analyzer (made in Germany). Thermogravimetric (TG) and differential scanning calorimetric (DSC) analyses were performed with an α-Al_2O_3 reference using a HCT-2 thermoanalyzer (Beijing Hengjun Instrument Co., PR China), at a heating rate of 10 °C/min from room temperature to 700 °C. Electronic micrographs were observed using a Shimadzu SS-550 scanning electron microscope (SEM) (made in Japan) operated at 15 kV and a JEOL JEM-1000 transmission electron microscope (TEM) (made in USA) operated at 200 kV, respectively. N_2 sorption isotherms were recorded on a Quantachrome NOVA 2000e sorption analyzer (made in USA) at liquid nitrogen temperature (77 K). Samples were degassed at 150 °C overnight prior to measurement. Surface areas were determined using the Brunauer–Emmett–Teller (BET) method, and pore size distributions were calculated using the Barrett–Joyner–Halenda (BJH) model. ^{13}C MAS-NMR and ^{31}P MAS-NMR spectra were recorded on a Bruker AV300 spectrometer (made in Germany). Test frequencies for ^{13}C MAS-NMR and ^{31}P MAS-NMR spectra were 78.20 and 121.49 MHz, respectively. The revolving speeds for ^{13}C MAS-NMR and ^{31}P MAS-NMR spectra were 8000 and 8192 Hz, respectively. The pulse widths for ^{13}C MAS-NMR and ^{31}P MAS-NMR experiments were 0.5 s. The relaxation times for ^{13}C MAS-NMR and ^{31}P MAS-NMR spectra were 0.5 and 10 s, respectively.

3. Results and discussion

3.1. Preparation and characterization of BHAZP

BHAZP was synthesized in the presence of BMTPA, $ZrOCl_2{\cdot}8H_2O$, SiF_4, and CTAB. The SEM image (Fig. 1a) shows that BHAZP has a regular film surface, and that the film is separated into numerous hexagonal plates. Edges and knots exist between the plates (Fig. 3d). After CTAB is extracted by ethanol, macropores of diameter ~200 nm are observed in the membrane (Fig. 1b), and the boundaries and knots between plates disappear. The TEM image (Fig. 1c) shows many mesopores of diameters ~19 nm in the walls of the macropores. This is consistent with the pore size distribution results (Fig. 2b) presented next.

Nitrogen adsorption–desorption isotherms of BHAZP and the corresponding pore size distribution are shown in Fig. 2a and b, respectively. Isotherms exhibiting behavior between those of types II and IV are characteristic of porous membranes, according to IUPAC classifications [21,22]. The adsorption curve for BHAZP rises slowly with minor adsorption at low to medium pressure, suggesting very little porosity on the microporous scale. The isotherm sharply increases at a relative pressure (P/P_0) of >0.9, which corresponds to accumulated pores. This indicates that there exists a secondary macroporous structure accompanied with mesopores, giving rise to capillary condensation between particles [23]. The wide hysteresis between the adsorption and desorption branches indicates a wide pore size distribution, corresponding to a macroporous structure [24]. A pore size distribution curve of BHAZP based on a BJH analysis is shown in Fig. 2b. The narrow peak at ~19 nm is characteristic of mesoporous structure.

An EXAPS analysis of the membranes composition in different areas is shown in Table 1. The average elemental percentages indicate no Si present in facial areas, except from in edges and knots between the hexagonal plates. The average Si and O contents of these edges are 37.35% and 40.55%, respectively, and of the knots are 39.38% and 38.24%, respectively. P and N are not detected, and only minor Zr and C contents are present in these areas. These